DESIGN FOR FERMILAB MAIN INJECTOR MAGNET RAMPS WHICH ACCOUNT FOR HYSTERESIS

B.C. Brown, C.M. Bhat, D.J. Harding, P.S. Martin, G. Wu
Fermi National Accelerator Laboratory *
Batavia, IL 60510-0500

Abstract

Although the dominant fields in accelerator electromagnets are proportional to the excitation current, precise control of accelerator parameters requires a detailed understanding of the fields in Main Injector[1][2]magnets including contribution from eddy currents, magnet saturation, and hysteresis. Operation for decelerating beam makes such considerations particularly significant. Analysis of magnet measurements and design of control system software is presented. Field saturation and its effects on low field hysteresis are accounted for in specifying the field ramps for dipole, quadrupole and sextupole magnets. Some simplifying assumptions are made which are accepted as limitations on the required ramp sequences. Specifications are provided for relating desired field ramps to required current ramps for the momentum, tune, and chromaticity control.

1 INTRODUCTION

Control of the momentum (p), tune (ν_x, ν_y) and chromaticity (ξ_x, ξ_y) of the accelerated beam is maintained through the interaction of several power supply systems and the rf system. Within the controls systems one must describe these variables as well as the currents and perhaps the voltages in the power supply loops. To simplify the interactions among these systems, we will rely on the beam variables rather than such secondary properties as the magnet currents or rf phases. This should allow us to deal with subtleties, such as the history dependent hysteresis of the magnets, in only one place.

We will relate these parameters to the fields of the primary magnet systems, ignoring contributions from correction and specialty magnets. The magnet systems[2]which must be considered in this context include the main dipole (IDA, IDB, IDC and IDD) system, the focusing and defocusing main quadrupole (IQB, IQC, IQD) systems, and the chromaticity sextupole (ISA) system which also has two families of sextupoles. We reference IDA, IQB and ISA magnet properties and design effective length ratios to prescribe the accelerator properties. The measured properties will be used to establish these parameters using suitable averages over all of the magnets in each circuit.

2 EQUATIONS

The equations will apply to particles on the design orbit which we will assume passes through the transverse centers of the dipole, quadrupole and sextupole magnets. If we integrate through the dipoles along a complete circumference C around the ring, the momentum, p, of the particles is

$$p = \frac{e}{2\pi}\int_C B_y\, ds = e(B\rho) \tag{1}$$

where e is the elementary charge, and B_y is the vertical component of the magnetic field. This expression defines $B\rho$ where ρ is a characteristic bending radius. We have $p = (e/\theta_D)B_1 L_{eff}$ for an IDA dipole which bends by $\theta_D = 2\pi/(30\,1/3)$,

The lattice design programs (such as MAD[3])describe the focusing properties of the lattice in terms of momentum-normalized gradients, k_1, and effective lengths, L_{eff} of the quadrupoles. If we take $k_{1f}(k_{1d})$ as the gradient in an IQB quadrupole on the focusing (defocusing) magnet circuit, we find the design betatron tunes (ν_x, ν_y) are given by

$$\begin{pmatrix}\nu_x\\ \nu_y\end{pmatrix} = \begin{pmatrix}Q_{11} & Q_{12}\\ Q_{21} & Q_{22}\end{pmatrix}\begin{pmatrix}k_{1f}\\ k_{1d}\end{pmatrix} \tag{2}$$

where $k_{1f}(k_{1d})$ is the design gradient for focusing (defocusing) IQB quadrupoles. We write this more compactly as $\underline{\nu} = \underline{Q}\,\underline{k_1}$. The similar description of the chromaticity[4],$\underline{\chi}$, must include not only the sextupole magnets but also the sextupole fields in the dipole magnets. We describe this using the normalized sextupole k_2 as $\underline{\chi} = \underline{\chi_0} + \underline{S_D}k_{2D} + \underline{S}\underline{k_2}$ or

$$\begin{pmatrix}\chi_x\\ \chi_y\end{pmatrix} = \begin{pmatrix}\chi_{x0}\\ \chi_{y0}\end{pmatrix} + \begin{pmatrix}S_{Dx}\\ S_{Dy}\end{pmatrix} k_{2D} + \begin{pmatrix}S_{11} & S_{12}\\ S_{21} & S_{22}\end{pmatrix}\begin{pmatrix}k_{2f}\\ k_{2d}\end{pmatrix}. \tag{3}$$

$\underline{\chi_0}$ is the natural chromaticity of the lattice, $k_{2f}(k_{2d})$ is the sextupole focusing near focusing (defocusing) quadrupole locations in the lattice, k_{2D} is the dipole contribution to sextupole expressed as the contribution of an IDA dipole. The column vector $\underline{S_D}$, and the matrices $\underline{Q}$ and $\underline{S}$ characterize the design lattice and are determined from lattice design programs.

For the quadrupoles, the relation between tune and focusing is not linear. Perturbations about the design $\underline{\nu}$ will require a different set of coefficients which can also be calculated from lattice simulations. We will therefore supplement $\underline{\nu} = \underline{Q}\,\underline{k_1}$ with $\delta\underline{\nu} = \delta\underline{Q}\,\delta\underline{k_1}$. $\delta\underline{\nu}$ is the (time dependent) difference between the tune specified in the base design and the tune desired by the machine operators, $\delta\underline{k_1}$ is the required change in the magnet focusing, and $\delta\underline{Q}$ expresses the coefficients for this differential change[1].

* Work supported by the U.S. Department of Energy under contract number DE-AC02-76CH03000.

[1] We also expect that the real machine will imperfectly match the simulations and may also express the measured tune *vs.* current differentials with an additional such equation.

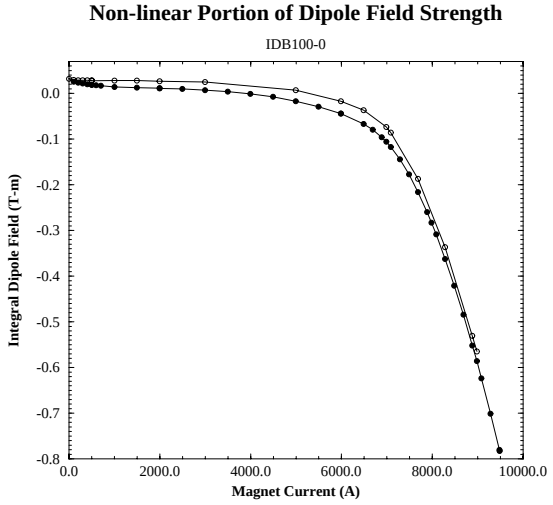

Figure 1: Nonlinear portion of integrated dipole strength for 6-m Main Injector dipole as measured by the Harmonics measuring system.

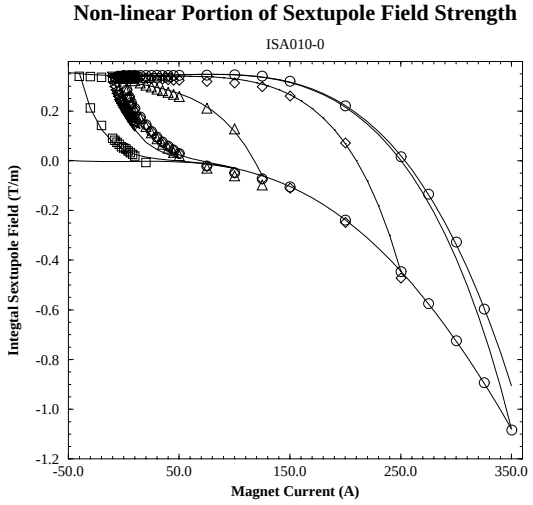

Figure 2: Nonlinear integral sextupole strength. Symbols represent measured data with a variety of ramps. Lines are analytic representations where $^{ramp}BL_N$ is represented by a 4th order polynomial and $^{trans}BL_N = (^{dn}BL_N - ^{up}BL_N)Exp(-|I - I_{reset}|/I_{char})$ with the up-down difference evaluated at the reset current. I_{char} is 20 A for up ramp transitions and 45 A for downramp transitions.

The focusing functions are defined in terms of the fields[2];

$$k_{N-1}L_{eff} = \frac{(N-1)\int B_N\, ds}{(B\rho)}. \quad (4)$$

The integrals are over a path along the transverse centerline and integrate through the length of the magnet. For the sextupole contribution of the dipole we have

$$k_{2D}L_D = \frac{2\int B_{3D}\, ds}{(B\rho)} = 2b_3\frac{\int B_{1D}\, ds}{(B\rho)a^2} = 2b_3\frac{\theta_D}{a^2}. \quad (5)$$

where the final expression employs the normalized sextupole harmonic to describe these fields.

Since we seek to specify the desired machine parameters and derive the required fields, we must invert these relations.

$$\underline{k_1} + \delta\underline{k_1} = \underline{Q}^{-1}\underline{\nu} + \delta\underline{Q}^{-1}\delta\underline{\nu}. \quad (6)$$

$$\underline{k_2} = \underline{S}^{-1}(\underline{\chi} - \underline{\chi_0} - \underline{S_D}2b_3\frac{\theta_D}{L_D a^2}). \quad (7)$$

3 SEXTUPOLE FROM DIPOLE MAGNETS

We neglect field errors (harmonics) except for the sextupole in the dipole magnets, described as $b_3 = b_3^{static} + b_3^{eddy}$.

The static sextupole field of the dipole magnets (measured at fixed current) is governed by a combination of the pole shape and contributions due to the iron. Measured hysteresis is negligible. b_3 measurements are obtained with two complimentary systems on each dipole[6].The contribution can be described either with a fitted function or a simple lookup table.

[2]Harmonic quadrupole fields, B_2, and sextupole fields, B_3 are defined following Glass[5].The factor of $N-1$ in the numerator is because MAD considers field derivatives rather than field harmonics as its basis of description.

The significant term due to eddy currents is created in the dipole beam pipe. Calculations[7]and measurements[8]have been carried out with rectangular shapes and with the actual beam pipe. Good agreement has been achieved. In the case of a rectangular approximation, the sextupole term is independent of the width of the pipe and the normalized sextupole harmonic is given by

$$b_3^{eddy} = \frac{\mu_0\sigma t a^2}{g}\frac{\dot{B}}{B} = P_{eddy}\frac{\dot{B}}{B} \quad (8)$$

where μ_0 and σ are the permeability and conductivity of the beam pipe material, t is the beam pipe thickness and g is the dipole gap height. $\dot{B}$ is the time derivative of the dipole field B. We use P_{eddy} to account for small corrections due the actual geometry.

4 CALCULATION OF REQUIRED FIELDS

Field integrals of a multipole electromagnet are given[9]by

$$B_N L_{eff} = \frac{\mu_0 N N_g L_{eff} I}{2A^N} - \frac{N\mathcal{L}L_{eff}}{2A^N}\mu_0 < H_{steel} > . \quad (9)$$

where N is the harmonic number (1 for dipole), N_g is the number of turns per gap in the coil, A the pole tip radius ($g/2$ for a dipole), $\mathcal{L}$ is the length of a flux line in iron with average H along the path of $<H_{steel}>$. I is the current through the coil. We note that the first term is proportional to I and it represents the field created in idealized iron by the magnet current. The second term describes the field lost in driving the iron. All saturation and hysteretic terms due to iron remanence are described by $<H_{steel}>$. In

Figs. 1 and 2 we show this quantity for the Main Injector dipole[9]and sextupole[10]magnets, respectively. Describing how these fields depend upon magnet excitation and excitation history is required to enable one to control the fields in situations where a variety of magnet ramp cycles are required.

These figures suggest that the iron can be driven to an up ramp (lower B field) hysteresis state or a down ramp (higher B field) hysteresis state. Reversing the sign of $\dot{B}$ by reversing $\dot{I}$ will begin a transition from one hysteretic state to the other. In accordance with Equation 9 we define the non-linear field integral, $(B_N L)_{nl}$, by

$$(B_N L_{eff})_{nl} = -\frac{N\mathcal{L}L_{eff}}{2A^{N-1}}\mu_0 < H_{steel} > \qquad (10)$$

$$= {}^{ramp}BL_N(I) - {}^{trans}BL_N(I - I_{rev}, I_{rev}) \qquad (11)$$

where the first term takes values of ${}^{up}BL_N(I)$ and ${}^{dn}BL_N(I)$ for up ramp and down ramp segments, ${}^{trans}BL_N(I - I_{rev}, I_{rev})$ describes the transition between the two hysteretic states, and I_{rev} is the current of the most recent reversal of $\dot{I}$. To describe the I required to produce a given B requires knowledge of the previous direction of the current ramp and the current level at which the most recent change of ramp direction occurred. These functions also have a weak dependence on the maximum and minimum currents in recent ramp cycles. In Fig. 2 we illustrate hysteresis curves using polynomial for the ramp state term and exponentials for the transition term.

5 RAMP CONTROL ISSUES

For the Fermilab Main Ring, one assumed that the momentum was proportional to the dipole current. Magnetic fields are scaled by momentum to set tune and chromaticity, while all the fields experience saturation and hysteresis. The addition of anti-proton deceleration cycles to the repertoire of the Main Injector makes hysteresis considerations especially significant and saturation at high fields is greater for Main Injector operation. Precise control of beam parameters requires a comprehensive new strategy.

Since the hysteresis effects depend on details of the ramp cycles, power supply control will be carried out by specifying the desired momentum (p), tune (ν_x, ν_y) and chromaticity (ξ_x, ξ_y) of the accelerated beam for a given operating mode, calculating the required fields, and determining current ramps in the 5 main current buses which achieve the required fields whenever beam is present. These calculations will be most effectively carried out in a single application which can then download the required current ramps to the real time power supply control system. In this fashion, the description of the hysteretic state is localized to an application program and is recalculated only when the operational requirements change. One may utilize special 'reset' ramp segments to establish a hysteretic state of magnets which simplifies efforts to match requirements over the balance of the cycle. Since we expect a mixture of 120 GeV and 150 GeV operating modes to be required in succession, we are concerned that a given mode may depend upon what current ramp was used in the previous mode. We will provide for a special reset segment at the end of each ramp cycle where each current bus can be required to execute some current changes which produce an approximately consistent magnetic state at the end of any magnet ramp.

6 LIMITATIONS AND ASSUMPTIONS

This model for power supply control assumes that the critical fields are controlled by these five magnet current systems and that the requirements depend only upon the specified beam quantities. It is known that the coherent Laslett tune shift[11]depends, instead, on the accelerated current in the ring. The tune control system will have to account for this in real time. Another exception is tune control for resonant extraction. But these need not upset the control of the hysteretic state which this system will achieve.

Other systems could affect the momentum, tune, and chromaticity. We assume that either by design or by operational control the dipole correctors and harmonic quadrupole correctors will not create net changes of p or ν.

7 REFERENCES

[1] Stephen D. Holmes. Status of the Main Injector and Recycler, Invited paper at PAC'97.

[2] *The Fermilab Main Injector Technical Design Handbook*. Fermilab (1994,1997).

[3] H. Grote and C. Iselin. The MAD Program Users Reference Guide. Sl 90-13(AP), CERN (1990).

[4] S.A. Bogacz and S. Peggs. Chromaticity Compensation - Main Injector Sextupole Strengths. Main Injector Note MI-0056, Fermilab (April 1991).

[5] Henry D. Glass, Measurement of Harmonic Amplitudes and Phases Using Rotating Coils. Technical Report MTF-94-0004 1.1, Fermilab (March 1994).

[6] D.J. Harding *et al*. Magnetic Field Measurements of the Initial Production Main Injector Dipoles. In *Proceedings of the 1995 IEEE Particle Accelerator Conference, Dallas, May 1-5, 1995*, p. 1340, Institute of Electrical and Electronic Engineers (1995).

[7] Jean-Francois Ostiguy. Eddy Current Induced Multipoles in the Main Injector. Main Injector Note MI-0037, Fermilab (October 1990).

[8] D.G. Walbridge *et al*. Measurements of Beam Pipe Eddy Current Effects in Main Injector Dipole Magnets. *Int. J. Mod. Phys. A (Proc. Suppl.)*, 2B:617 (1993).

[9] B.C. Brown *et al*. Results on Fermilab Main Injector Dipole Measurements. *IEEE Trans. on Magnetics*, 32:2186 (1996).

[10] C.M. Bhar *et al*. Magnetic Field Measurements of the Main Injector Sextupole Magnets (PAC'97).

[11] C. Moore, R. Gerig and S. Pruss. Measurement and Compensation of Coherent Laslett Tune Shifts in the Fermilab Main Ring. *IEEE Transactions on Nuclear Science*, NS-28:2486 (1981). 1981 Particle Accelerator Conference.